Theoretical Study of Rhenium Dinuclear Complexes: Re−Re Bonding Nature and Electronic Structure

Ken Saito,[†] Yoshihide Nakao,[†] Hirofumi Sato,[†] and Shigeyoshi Sakaki*[,†,‡]

Department of Molecular Engineering, Graduate School of Engineering, Kyoto University, Nishikyo-ku, Kyoto 615-8510, Japan, and Fukui Institute for Fundamental Chemistry, Nishihiraki-chou, Takano, Sakyo-ku, Kyoto 606-8103, Japan

Received: December 29, 2005; In Final Form: March 24, 2006

Four dinuclear rhenium complexes, $[Re_2Cl_8]^{2-}$ (**1**), $[Re_2(\mu\text{-}Cl)_3Cl_6]^{2-}$ (**2a**), $[Re_2(\mu\text{-}Cl)_3Cl_6]^{-}$ (**2b**), and $[Re_2(\mu\text{-}Cl)_2Cl_8]^{2-}$ (**3**), were theoretically investigated by the CASSCF, MRMP2, SA-CASSCF, and MCQDPT methods. Interesting differences in electronic structure and Re−Re bonding nature among these complexes are clearly reported here, as follows: In **1**, the ground state is the $^1A_{1g}$ state. The approximate stabilization energies by the σ, π, and δ bonding interactions are evaluated to be 4.36, 2.89, and 0.52 eV, respectively, by the MRMP2 method. In **2a**, the ground state is the $^2E''$ state. The approximate stabilization energy by two degenerate δ bonding interactions is estimated to be 0.36 eV by the MCQDPT method. One δ bonding interaction of **2a** is much weaker than that of **1**, which is discussed in terms of the Re−Re distance and the Re oxidation state. In **2b**, the ground state is the $^1A_1'$ state, of which multiconfigurational nature is extremely large unlike that of the $^2E''$ ground state of **2a** despite similarities between **2a** and **2b**. In **3**, the σ, π, and δ bonding interactions are not effectively formed between two Re centers. As a result, the ^1A_g, $^3B_{1u}$, ^5A_g, and $^7B_{1u}$ states are in almost the same energy within 0.03 eV. This result is consistent with the paramagnetism of **3** experimentally reported.

1. Introduction

$[Re_2Cl_8]^{2-}$ (d^4-d^4) (**1**; see Chart 1) is one of the most interesting dinuclear transition metal complexes, because this complex possesses a unique Re−Re quadruple bond in a formal sense, as reported by Cotton and his collaborators.[1] In this complex, the $d_{x^2-y^2}$ orbital of each Re center interacts with Cl ligands and the other four d orbitals participate in the Re−Re bonding and antibonding molecular orbitals, as follows: Two d_{z^2} orbitals interact with each other to form $\sigma(a_{1g})$ and $\sigma^*(a_{2u})$ molecular orbitals, as shown in Chart 2. The d_{xz} and d_{yz} orbitals of one Re center interact with those of the other Re center to form $\pi(e_u)$ and $\pi^*(e_g)$ molecular orbitals. The d_{xy} orbital of one Re center interacts with that of the other Re center to form δ-(b_{2g}) and $\delta^*(b_{1u})$ molecular orbitals. The quadruple Re−Re bond arises from the $\sigma^2\pi^4\delta^2$ electron configuration.[1] The eclipsed structure with D_{4h} symmetry of this complex is one of the evidences of the presence of the δ bonding interaction; if this bonding interaction was absent, the eclipsed structure became less stable than the staggered one because of the larger static repulsion between Cl ligands.[1] Similar complexes such as $[Mo_2Cl_8]^{4-}$, $[Tc_2Cl_8]^{2-}$, and $[Tc_2Cl_8]^{3-}$ have been reported so far.[2−4] Their metal−metal bonding nature is discussed in the same way.

Several rhenium dinuclear complexes taking different structures from that of **1** have been reported so far. Some of them are $[Re_2(\mu\text{-}Cl)_3Cl_6]^{2-}$ (d^3-d^4) (**2a**) and $[Re_2(\mu\text{-}Cl)_3Cl_6]^{-}$ (d^3-d^3) (**2b**), which take a face-sharing bioctahedral structure with D_{3h} symmetry,[5−7] as shown in Chart 1. In these complexes, five d orbitals of each Re center split into e_g- and t_{2g}-like orbitals.

CHART 1: Structures of Rhenium Dinuclear Complexes Examined Here

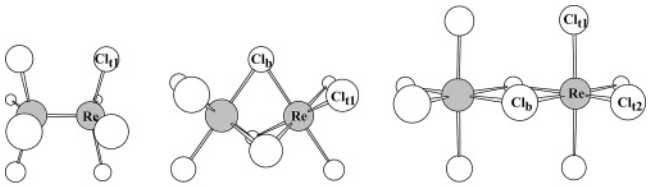

$[Re_2Cl_8]^{2-}$ (**1**) $[Re_2(\mu\text{-}Cl)_3Cl_6]^{2-}$ (**2a**) $[Re_2(\mu\text{-}Cl)_3Cl_6]^{-}$ (**2b**) $[Re_2(\mu\text{-}Cl)_2Cl_8]^{2-}$ (**3**)

The former orbitals are unoccupied in a formal sense because they are at much higher energy than the latter orbitals by the antibonding interaction with Cl ligands. The latter orbitals form $\sigma(a_1')$, $\delta(e')$, $\delta^*(e'')$, and $\sigma^*(a_2'')$ molecular orbitals between two Re centers, as shown in Chart 3. This means that these complexes contain a Re−Re multiple bond in a formal sense. Similar complexes such as $[Ti_2(\mu\text{-}Cl)_3Cl_6]^{-}$, $[Cr_2(\mu\text{-}Cl)_3Cl_6]^{3-}$, $[Mo_2(\mu\text{-}Cl)_3Cl_6]^{3-}$, and $[W_2(\mu\text{-}Cl)_3Cl_6]^{3-}$ have been reported, too.[8−11] Another example is $[Re_2(\mu\text{-}Cl)_2Cl_8]^{2-}$ (d^3-d^3) (**3**), which takes an edge-sharing bioctahedral structure with D_{2h} symmetry, as shown in Chart 1.[12] Like **2a** and **2b**, five d orbitals of each Re center split into e_g- and t_{2g}-like orbitals. The former orbitals are unoccupied like those in **2a** and **2b**. The latter orbitals form $\sigma(a_g)$, $\pi(b_{2u})$, $\delta(b_{1g})$, $\delta^*(a_u)$, $\pi^*(b_{3g})$, and $\sigma^*(b_{1u})$ molecular orbitals between two Re centers, as shown in Chart 4. $[Ti_2(\mu\text{-}Cl)_2Cl_8]^{2-}$, $[Mo_2(\mu\text{-}Cl)_2Cl_8]^{2-}$, and $[Re_2(\mu\text{-}Cl)_2Cl_8]$ also take a similar edge-sharing bioctahedral structure.[8,13,14]

Many theoretical studies of **1** have been carried out to clarify its interesting electronic structure and its Re−Re bonding nature.[15−18] However, the $^1A_{1g} \rightarrow {}^1A_{2u}$ ($\delta \rightarrow \delta^*$) excitation energy was not correctly calculated previously; for instance,

* Corresponding author. E-mail: sakaki@moleng.kyoto-u.ac.jp.
[†] Kyoto University.
[‡] Fukui Institute for Fundamental Chemistry.

10.1021/jp057558j CCC: $33.50 © 2006 American Chemical Society
Published on Web 07/14/2006

CHART 2: Re−Re Bonding and Antibonding Orbitals of $[Re_2Cl_8]^{2-}$ (1)

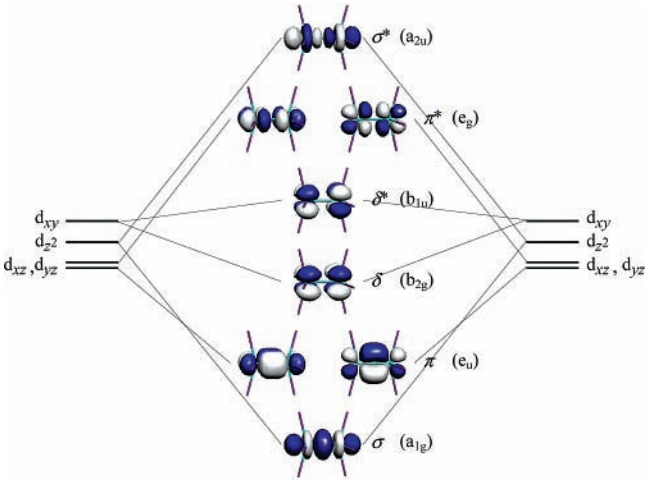

CHART 3: Re−Re Bonding and Antibonding Orbitals of $[Re_2(\mu\text{-}Cl)_3Cl_6]^{2-}$ (2a) and $[Re_2(\mu\text{-}Cl)_3Cl_6]-$ (2b)

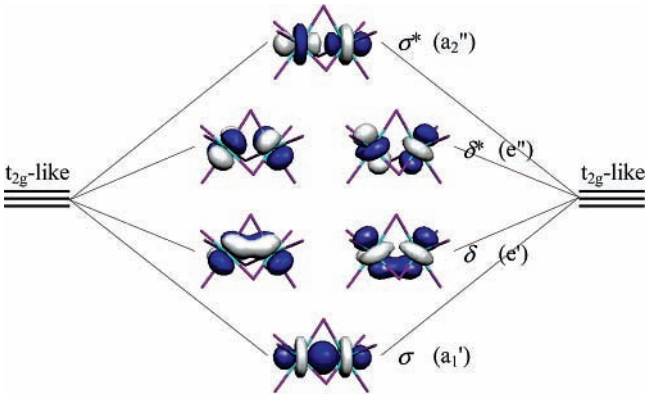

CHART 4: Re−Re Bonding and Antibonding Orbitals of $[Re_2(\mu\text{-}Cl)_2Cl_8]^{2-}$ (3)

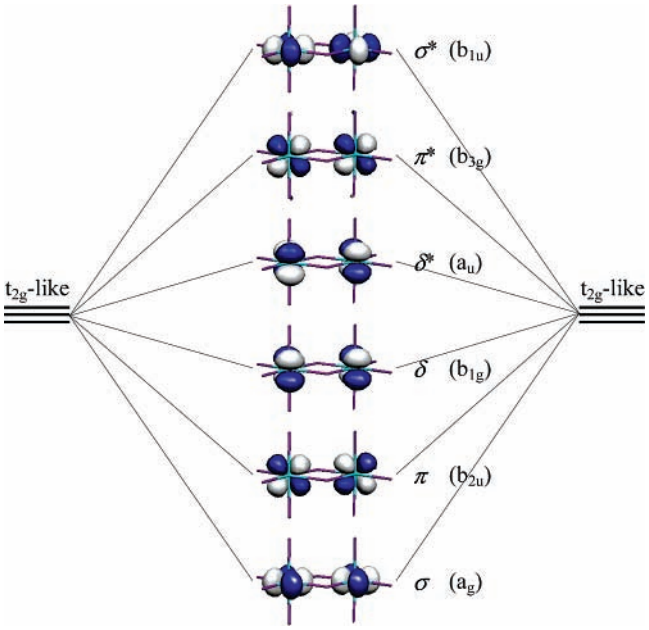

the self-consistent-field Xα scattered-wave (SCF-Xα-SW) method presented a much smaller excitation energy (0.87 eV)[15] than the experimental value (1.82 eV).[19] On the other hand, the general valence bond method with the configuration interaction (GVB-CI) and the complete active space self-consistent-field (CASSCF) method presented large excitation energies, 3.20[16] and 3.384 eV,[17] respectively. Recently, its excitation energy was correctly evaluated to be 1.97 eV by the second-order perturbation theory based on the CASSCF reference state (CASPT2).[18] This result suggests that incorporation of dynamical electron correlation based on the multireference wave function is indispensable to investigate this complex.

Various kinds of face- and edge-sharing dinuclear metal complexes including **2a**, **2b**, and **3** were also theoretically investigated with the broken-symmetry density functional theory (BS-DFT) by Stranger and his collaborators,[20] in which metal−metal bonding nature was discussed. However, the relative energies of several important electronic states have not been studied yet, although they deeply relate to the metal−metal bonding nature. It is worthwhile to evaluate the relative energies of the ground and several low-energy excited states of these dinuclear rhenium complexes and to shed clear light on the Re−Re bonding nature.

In this work, we theoretically investigated **1**, **2a**, **2b**, and **3** with the multireference second-order Møller−Plesset perturbation theory (MRMP2)[21] and the multiconfigurational quasi-degenerate second-order perturbation theory (MCQDPT).[22] Our purposes here are to show clearly what is the ground state, to evaluate relative energies of several important low-energy excited states and to clarify electronic structures and Re−Re bonding nature of these complexes. The DFT(B3LYP),[23,24] coupled cluster singles and doubles with perturbative triples (CCSD(T)), BS-DFT(B3LYP), and BS-CCSD(T) methods were also applied to **1** and **2b** to examine reliabilities of these methods for theoretical investigation of these dinuclear rhenium complexes.

2. Computational Details

Geometries of these complexes were taken from X-ray analyses (see Table S1 in Supporting Information).[1,5,12] Only in **1** was geometry optimization performed with the CASSCF and MRMP2 methods, where the Re−Re and Re−Cl_{t1} bond distances and the Re−Re−Cl_{t1} bond angle were optimized under D_{4h} symmetry. Potential energy curve (PEC) of **1** was evaluated with the MRMP2 method, where the only Re−Re bond distance was changed but the Re−Cl_{t1} bond distance and Re−Re−Cl_{t1} bond angle were fixed to the corresponding experimental values, respectively.

We employed two basis set systems (basis I and II) in this study. In basis I, core electrons of Re were replaced with the small relativistic effective core potentials (ECPs) reported by Hay and Wadt[25] and valence electrons were represented by a (541/541/111/1) basis set.[25−27] The cc-pVDZ basis set was used for Cl.[28] In basis II, valence electrons of Re were represented by a (4311/4311/111/1) basis set,[25−27] whereas the same ECPs as those of basis I were used to replace core electrons. For Cl, the aug-cc-pVDZ basis set[28] was used.

The CASSCF and MRMP2 methods were applied to **1**, **2b**, and **3** to investigate their nondegenerate electronic states, and the state-averaged CASSCF (SA-CASSCF) and MCQDPT methods were applied to **2a** to investigate its degenerate electronic states. In the CASSCF calculation of **1**, one σ, two π, and one δ molecular orbitals and their antibonding counterparts were taken as the active space (see Chart 2), in which eight electrons were involved. Molecular orbitals that consist mainly of the $d_{x^2-y^2}$ orbital were excluded from the active space because they are at much different energies from the active orbitals. In the SA-CASSCF calculation of **2a** and the CASSCF

TABLE 1: Optimized Re−Re and Re−Cl_{t1} Bond Distances (in Å) and Re−Re−Cl_{t1} Bond Angle (in deg) of $[Re_2Cl_8]^{2-}$ (1)

method	r(Re−Re)	r(Re−Cl_{t1})	a(Re−Re−Cl_{t1})	
CASSCF	2.259	2.382	104.7	this work (basis I)
	2.260	2.381	104.6	this work (basis II)
MRMP2	2.236	2.342	103.8	this work (basis I)
	2.250	2.341	103.1	this work (basis II)
CASPT2	2.259	2.304	103.44	ref 18
exptl.	2.24	2.29	103.7	ref 1

calculation of **2b**, one σ and two δ molecular orbitals and their antibonding counterparts were taken as the active space (Chart 3).[29] Seven and six electrons were involved in the active spaces of **2a** and **2b**, respectively. In the CASSCF calculation of **3**, one σ, one π, and one δ molecular orbitals and their antibonding counterparts were taken as the active space (Chart 4), in which six electrons were involved. Molecular orbitals that consist mainly of the e_g-like d orbitals were excluded from the active space of **2a**, **2b**, and **3** because they are at much different energies from the active orbitals. The MRMP2 and MCQDPT calculations were carried out with the reference wave function from the CASSCF and SA-CASSCF calculations, respectively. In these calculations, the 1s, 2s, and 2p orbitals of Cl ligand were kept to be frozen.

The CASSCF and SA-CASSCF calculations were performed with the GAMESS program package.[30] The MRMP2 and MCQDPT calculations were carried out with the MR2D program[31] implemented in the GAMESS package. The DFT(B3LYP), CCSD, CCSD(T), BS-DFT(B3LYP), BS-CCSD, and BS-CCSD(T) calculations were performed with the Gaussian 03 (revision C.02) program package.[32] Molecular orbitals were drawn by the MOLEKEL (version 4.3) program.[33]

3. Results and Discussions

3.1. $[Re_2Cl_8]^{2-}$ (1) with a Re−Re Direct Bond. The geometry of **1** in the $^1A_{1g}$ ground state was optimized with the CASSCF and MRMP2 methods, as shown in Table 1. At the CASSCF level of theory with both basis I and basis II, the optimized Re−Re distance and Re−Re−Cl_{t1} angle are in good agreement with the experimental values, whereas the optimized Re−Cl_{t1} distance is somewhat longer than the experimental value. All these geometrical parameters are improved at the MRMP2 level of theory; the Re−Re distance and the Re−Re−Cl_{t1} angle are almost the same as their experimental values and the Re−Cl_{t1} distance considerably approaches its experimental value. Thus, the MRMP2 method reproduces well the geometry of **1** like the CASPT2 method.[18]

Relative energies and natural orbital populations of several important electronic states were evaluated by the CASSCF/basis II and MRMP2/basis II methods with the experimental geometry, as shown in Table 2. In the $^1A_{1g}$ ground state, the population of the δ orbital (1.52) is much smaller than the usual value (2.0) of a doubly occupied orbital and that of the δ^* orbital (0.48) is much larger than the usual value (0.0) of an unoccupied orbital. These results suggest that the δ bonding interaction is very weak. Therefore, the multireference theoretical method should be applied to this complex. Actually, the weights of the main configuration ($\sigma^2\pi^4\delta^2$) and the second leading one ($\sigma^2\pi^4\delta^{*2}$) are evaluated to be 67 and 18%, respectively, by the CASSCF method. Almost the same results were presented with the MRMP2-optimized geometry (see Table S2 in Supporting Information). Also, it is noted that both basis I and II present almost the same optimized geometries, relative energies and natural orbital populations, suggesting the reliability of these basis set systems; see Tables 1 and 2 and Supporting Information Table S2.

The natural orbital populations of the σ, π, and δ bonding orbitals are much larger than those of their antibonding counterparts, respectively, in the $^1A_{1g}$ ground state, as shown in Table 2. This result suggests that all σ, π, and δ bonding interactions contribute to the Re−Re bond. From these natural orbital populations, the Re−Re bond order[34] is evaluated to be 3.18 in the $^1A_{1g}$ ground state, which is much smaller than 4.0. This value is almost the same as the previous value (3.20) evaluated by the CASPT2 method.[18] In the $^3A_{2u}$ excited state, on the other hand, the population of the δ orbital is almost the same as that of the δ^* orbital, whereas the populations of the σ, σ^*, π, and π^* orbitals in the $^3A_{2u}$ state are almost the same as those in the $^1A_{1g}$ state, respectively. This means that the δ bonding interaction disappears upon going to the $^3A_{2u}$ state from the $^1A_{1g}$ state, and that the energy difference between these two states corresponds to the approximate stabilization energy by the δ bonding interaction.[35,36] This energy difference is estimated to be 0.52 eV by the MRMP2 method. In the $^7A_{2u}$ state,[37] the population of the σ orbital is larger than that of the σ^* orbital and the populations of the π and δ orbitals are almost the same as those of the π^* and δ^* orbitals, respectively, as shown in Table 2. This means that only one σ bonding interaction remains but the π and δ bonding interactions disappear in the $^7A_{2u}$ state. Thus, the energy difference between the $^7A_{2u}$ and $^3A_{2u}$ states is the approximate stabilization energy by the two components of degenerate π bonding interactions. This energy difference is evaluated to be 5.77 eV by the MRMP2 method.[36] In the $^9A_{1g}$ state,[37] the populations of the σ, σ^*, π, π^*, δ, and δ^* orbitals are 1.00, which means that all Re−Re bonding interactions disappear. The energy difference between the $^7A_{2u}$ and $^9A_{1g}$ states corresponds to the approximate stabilization energy by the σ bonding interaction. This energy difference is evaluated to be 4.36 eV by the MRMP2 method.[36] These results are summarized, as follows: The σ, π, and δ bonding interactions yield the approximate stabilization energies 4.36, 2.89 (=5.77/2), and 0.52 eV, respectively; note that two π bonds exist. The δ bonding interaction is much weaker than the π bonding interaction and the π bonding interaction is much weaker than the σ bonding interaction, as expected. Although this result is not surprising, this is the first semiquantitative estimation of relative strengths of the σ, π, and δ bonding interactions of **1**.

The $^1A_{1g} \rightarrow {}^1A_{2u}$ ($\delta \rightarrow \delta^*$) excitation energy is evaluated to be 3.14 and 1.95 eV by the CASSCF and MRMP2 method, respectively. It is noted that although the CASSCF-calculated value is much larger than the experimental value (1.82 eV)[19] like the previous CASSCF-evaluated value,[17] the MRMP2-calculated value agrees well with the experimental value like the CASPT2-calculated value.[18] This result indicates that incorporation of dynamical electron correlation based on the multireference wave function is indispensable, as reported.[18]

The PECs of the $^1A_{1g}$, $^3A_{2u}$, $^7A_{2u}$, and $^9A_{1g}$ states were calculated by the MRMP2/basis II method, as shown in Figure 1; almost the same PECs were presented by the MRMP2/basis I method, too (see Figure S1 in Supporting Information).[38] The Re−Re distance at the energy minimum relates to the strength of the Re−Re bonding interaction. The energy minimum of the $^3A_{2u}$ state is at a slightly longer Re−Re distance (2.3 Å) than that of the $^1A_{1g}$ state (2.2 Å). Also, the shapes of the PECs of these two states resemble each other. These results arise from the fact that the weak δ bonding interaction disappears upon going to the $^3A_{2u}$ state from the $^1A_{1g}$ state. In

TABLE 2: Relative Energies (in eV) and Natural Orbital Populations[a,b] of Several Important States of $[Re_2Cl_8]^{2-}$ (1), $[Re_2(\mu\text{-}Cl)_3Cl_6]^{2-}$ (2a), $[Re_2(\mu\text{-}Cl)_3Cl_6]^{-}$ (2b), and $[Re_2(\mu\text{-}Cl)_2Cl_8]^{2-}$ (3)

		relative energy			natural orbital population					
complex	state	CASSCF	MRMP2	exptl	σ	σ^*	π	π^*	δ	δ^*
1	$^1A_{1g}$	0.00	0.00		1.92	0.08	3.74	0.26	1.52	0.48
	$^3A_{2u}$	0.45	0.52		1.92	0.08	3.75	0.25	1.01	0.99
	$^7A_{2u}$	5.97	6.29		1.90	0.10	2.02	1.98	1.00	1.00
	$^9A_{1g}$	9.68	10.65		1.00	1.00	2.00	2.00	1.00	1.00
	$^1A_{2u}$	3.14	1.95	1.82[19]	1.92	0.08	3.70	0.30	1.04	0.96
		relative energy			natural orbital population					
complex	state	SA-CAS	MCQDPT	exptl	σ	σ^*	π	π^*	δ	δ^*
2a	$^2E''$	0.00	0.00		1.87	0.13			3.47	1.53
	$^4E'$	0.34	0.36		1.87	0.13			2.93	2.07
		relative energy			natural orbital population					
complex	state	CASSCF	MRMP2	exptl	σ	σ^*	π	π^*	δ	δ^*
2b	$^1A_1'$	0.00	0.00		1.62	0.38			2.18	1.82
	$^3A_2''$	0.08	0.07		1.62	0.38			2.12	1.88
	$^5A_1'$	0.26	0.21		1.62	0.38			2.01	1.99
	$^7A_2''$	1.09	1.94		1.00	1.00			2.00	2.00
3	^1A_g	0.02	0.03		1.00	1.00	0.99	1.01	0.97	1.03
	$^3B_{1u}$	0.02	0.02		1.00	1.00	0.99	1.01	0.97	1.03
	^5A_g	0.01	0.02		1.00	1.00	0.99	1.01	0.98	1.02
	$^7B_{1u}$	0.00	0.00		1.00	1.00	1.00	1.00	1.00	1.00

[a] Basis II was used. [b] Natural orbital populations of **1**, **2b**, and **3** were evaluated by the CASSCF method and those of **2a** were evaluated by the SA-CASSCF method.

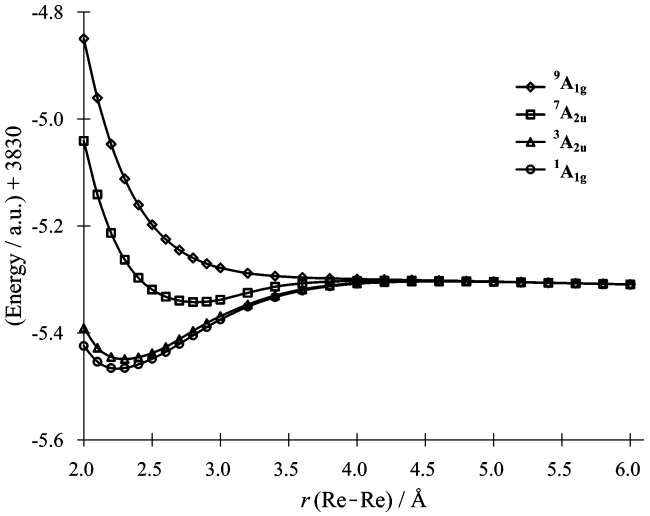

Figure 1. Potential energy curves of the $^1A_{1g}$, $^3A_{2u}$, $^7A_{2u}$, and $^9A_{1g}$ states of $[Re_2Cl_8]^{2-}$ (**1**). Basis II was used.

contrast, the energy minimum of the $^7A_{2u}$ state is at a much longer Re−Re distance (2.8 Å) than that of the $^3A_{2u}$ state (2.3 Å). Also, it is noted that the PEC of the $^7A_{2u}$ state is very shallow, unlike those of the $^1A_{1g}$ and $^3A_{2u}$ states. These results are interpreted in terms that the stronger π bonding interaction disappears upon going to the $^7A_{2u}$ state from the $^3A_{1g}$ state. The PEC of the $^9A_{1g}$ state is completely repulsive because all Re−Re bonding interactions are absent in this state.

Natural orbital populations of the σ, π, δ, δ^*, π^*, and σ^* orbitals evaluated by the CASSCF/basis II method are presented as a function of the Re−Re distance in Figure 2a−c. In the $^1A_{1g}$ state, the population of the δ orbital becomes almost the same as that of the δ^* orbital at r(Re−Re) = 3.6 Å, as shown in Figure 2a; in other words, the δ bonding interaction disappears at this distance. On the other hand, the populations of the σ and π bonding orbitals are still larger than those of their antibonding counterparts, respectively, even when the Re−Re distance is longer than 3.6 Å. This result indicates that the σ and π bonding interactions still remain in this region. They disappear at r(Re−Re) = 4.6 and 6.0 Å, respectively. These results are useful to discuss what type of interaction contributes to the metal−metal bond in dinuclear metal complexes.

Energy differences between the $^1A_{1g}$ and $^3A_{2u}$ states and between the $^1A_{1g}$ and $^1A_{2u}$ states were also investigated by the DFT(B3LYP), CCSD, CCSD(T), BS-DFT(B3LYP), BS-CCSD, and BS-CCSD(T) methods, as shown in Table 3. The $^3A_{2u}$ state is calculated to be more stable than the $^1A_{1g}$ state by the DFT-(B3LYP) and CCSD methods. This result is completely different from the relative stability calculated by the MRMP2 method.[39] On the other hand, the CCSD(T) and all BS methods present the correct stability order of these three states. These results indicate that the BS-DFT(B3LYP), BS-CCSD, and BS-CCSD-(T) methods are useful to discuss bonding nature and the electronic state of the ground state in this complex, as reported previously.[20]

3.2. Face-Sharing Complexes, $[Re_2(\mu\text{-}Cl)_3Cl_6]^{2-}$ (2a) and $[Re_2(\mu\text{-}Cl)_3Cl_6]^{-}$ (2b). In **2a**, the $^2E''$ and $^4E'$ states were investigated by the SA-CASSCF and MCQDPT methods because both states are degenerate. The $^2E''$ state is the ground state and the $^4E'$ excited state is calculated to be 0.36 eV above the $^2E''$ state by the MCQDPT/basis II method, as shown in Table 2; almost the same results are calculated with basis I (see Supporting Information Table S3). In the $^2E''$ state, the natural orbital populations of the δ and δ^* orbitals are 3.47 and 1.53, respectively. These values are much different from formal values (4.0 and 1.0 for the δ and δ^* orbitals, respectively) in the pure $\sigma^2\delta^4\delta^{*1}$ configuration. This result suggests that the electronic structure of **2a** cannot be described well by one $\sigma^2\delta^4\delta^{*1}$ configuration. Actually, the weights of this configuration and the second leading one ($\sigma^2\delta^2\delta^{*3}$) are evaluated to be 72 and 12%, respectively, by the SA-CASSCF method. Consistent with these results, the Re−Re bond order is only 1.84, which is much smaller than the formal value (2.5) in the pure $\sigma^2\delta^4\delta^{*1}$ configuration.

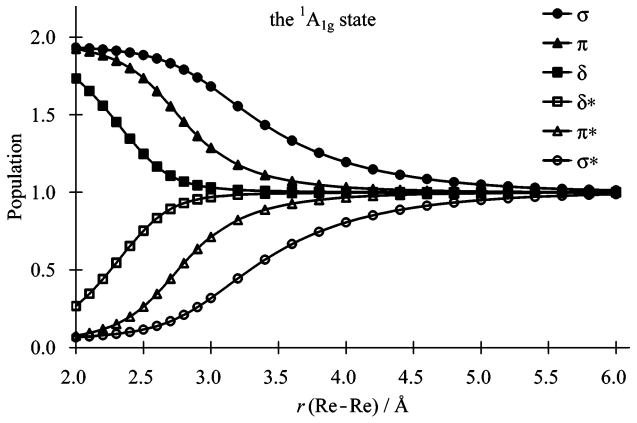

(a) the $^1A_{1g}$ state

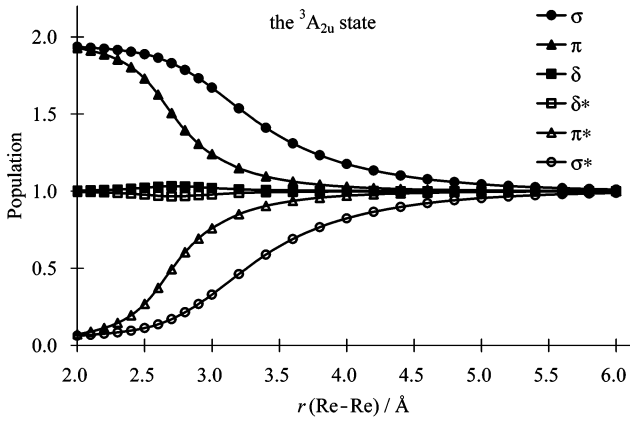

(b) the $^3A_{2u}$ state

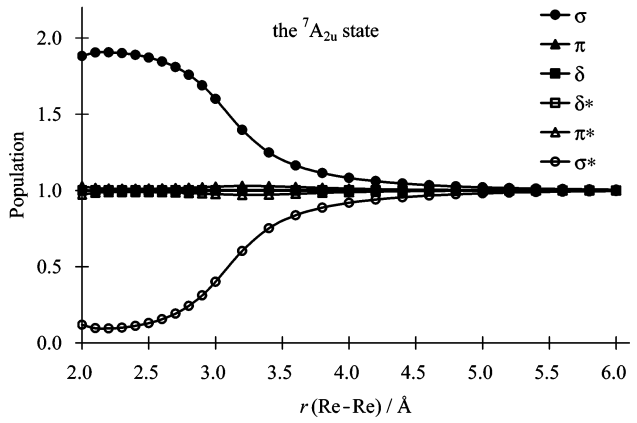

(c) the $^7A_{2u}$ state

Figure 2. Natural orbital populations of the σ, π, δ, δ^*, π^*, and σ^* orbitals in the $^1A_{1g}$, $^3A_{2u}$, and $^7A_{2u}$ states of $[Re_2Cl_8]^{2-}$ (**1**). Basis II was used.

In the $^4E'$ excited state, the populations of the δ and δ^* orbitals are 2.93 and 2.07, respectively; note the δ and δ^* orbitals are doubly degenerate (see Chart 3). Because the difference between these two populations (0.86) is much smaller than that in the $^2E''$ state (1.94) by about 1, the δ bonding interaction in the $^4E'$ state is much weaker than that in the $^2E''$ state. The populations of the σ and σ^* orbitals are little different between these two states. Thus, the energy difference (0.36 eV) between these two states corresponds to the approximate stabilization energy by the two components of degenerate δ bonding interactions. These δ bonding interactions are much weaker than that of **1**. Its reason is easily understood in terms of the Re−Re distance and the Re oxidation state. In **2a**, the Re−Re distance is much longer than that of **1** because of the face-sharing bioctahedral geometry. Also, **2a** consists of Re(III) and Re(IV) centers, and **1** consists of two Re(III) centers. Because the d orbital of Re(IV) expands less than that of Re(III), the $d_\delta-d_\delta$ overlap of **2a** is smaller than that in **1**. Because of these two factors, the δ bonding interaction is weaker in **2a** than in **1**.

Relative energies and natural orbital populations of the other face-sharing rhenium complex (**2b**) were investigated by the CASSCF/basis II and MRMP2/basis II methods, as shown in Table 2; basis I presents almost the same results as basis II (see Supporting Information Table S3). The $^1A_1'$ state is the ground state and the $^3A_2''$ and $^5A_1'$ excited states are evaluated to be at slightly higher energies than the ground state with the MRMP2 method by 0.07 and 0.21 eV, respectively (see Table 2). The $^7A_2''$ excited state is at much higher energy than the $^5A_1'$ state by 1.73 eV.

In the $^1A_1'$ ground state, the populations of the δ and δ^* orbitals are 2.18 and 1.82, respectively (see Table 2), which clearly shows that the δ bonding interaction is very weak because both populations are close to each other. This means that a multireference method such as MRMP2 or CASPT2 should be employed to investigate **2b** like **1** and **2a**. Actually, the weight of the main configuration ($\sigma^2\delta^4$) is evaluated to be very small (18%) by the CASSCF method; the weights of the other configurations are smaller than 14% (see Table S4 in Supporting Information). Consistent with the very small weight of the $\sigma^2\delta^4$ configuration, the Re−Re bond order is only 0.80. In the $^5A_1'$ excited state, the populations of the δ and δ^* orbitals are 2.01 and 1.99, respectively. This means that the δ bonding interaction is negligibly small in this state. The energy difference between the $^1A_1'$ and $^5A_1'$ states is evaluated to be 0.21 eV by the MRMP2 method, which corresponds to the approximate stabilization energy by the two components of degenerate δ bonding interactions.

The strength of the σ bonding interaction in **2b** is also worthy of investigation. The populations of the σ and σ^* orbitals are 1.62 and 0.38, respectively, in both the $^1A_1'$ and $^5A_1'$ states, as shown in Table 2. These values suggest that the σ bonding interaction is not strong very much unlike those of **1** and **2a**. In the $^5A_1'$ state, the weights of the $\sigma^2\delta^2\delta^{*2}$ and $\delta^2\delta^{*2}\sigma^{*2}$ configurations are evaluated to be 73 and 11%, respectively, by the CASSCF method. In the $^7A_2''$ state, the population of the σ orbital is the same as that of the σ^* orbital, which indicate that even the σ bonding interaction disappears in this state. Thus, the energy difference between the $^5A_1'$ and $^7A_2''$ states (1.73 eV) corresponds to the approximate stabilization energy by the σ bonding interaction, which is much smaller than that (4.36 eV) of **1**. The σ bond order in the $^1A_1'$ state of **2b** (0.62) is also considerably smaller than those in the $^1A_{1g}$ state of **1** (0.92) and the $^2E''$ state of **2a** (0.87). This weak σ bond of **2b** is interpreted, as follows: One factor is the long Re−Re distance; because the Re−Re distance of **2b** (2.704 Å) is much longer than that of **1** (2.24 Å), the $d_\sigma-d_\sigma$ overlap between two Re centers is much smaller in **2b** than in **1**. The other factor is the oxidation state of the Re center. In **1**, the populations of the σ and σ^* orbitals are 1.83 and 0.17, respectively, when the Re−Re distance is taken to be the same as the experimental distance (2.704 Å) of **2b**, as shown in Figure 2a. Thus, the σ bond order of **1** with this Re−Re distance is 0.83, which is considerably larger than that of **2b** (0.62), even though the Re−Re distance is the same. This result clearly shows that not only the Re−Re

TABLE 3: Comparisons of DFT(B3LYP), CCSD, CCSD(T), BS-DFT(B3LYP), BS-CCSD, and BS-CCSD(T) Methods in Calculating Relative Energies of the $^1A_{1g}$, $^3A_{2u}$, and $^1A_{2u}$ States of $[Re_2Cl_8]^{2-}$ (1) and Those of the $^1A_1'$ and $^5A_1'$ States of $[Re_2(\mu\text{-}Cl)_3Cl_6]^-$ (2b)

complex	state	B3LYP	CCSD	CCSD(T)	BS-B3LYP	BS-CCSD	BS-CCSD(T)	exptl
				basis I				
1	$^1A_{1g}$	0.00	0.00	0.00	0.00	0.00	0.00	0.00
	$^3A_{2u}$	−0.30	−0.51	0.10	0.18	0.32	0.20	
	$^1A_{2u}$	0.70	0.80	0.69	1.18	1.61	0.62	1.82[19]
2b	$^1A_1'$	0.00	0.00	0.00	0.00	0.00	0.00	
	$^5A_1'$	−1.83	−2.48	−2.25	0.14	−0.84	−0.66	
				basis II				
1	$^1A_{1g}$	0.00	0.00	0.00	0.00			0.00
	$^3A_{2u}$	−0.27	−0.49	0.15	0.19			
	$^1A_{2u}$	0.73	0.83	0.72	1.18			1.82[19]
2b	$^1A_1'$	0.00	0.00	0.00	0.00			
	$^5A_1'$	−1.79	−2.49	−2.25	0.15			

distance but also the other factor are responsible for the weaker σ bond of **2b** than that of **1**. Such a factor is the oxidation state of the Re center. As discussed above, **1** consists of two Re(III) atoms, but **2b** consists of two Re(IV) atoms. The less-expanding d orbital of Re(IV) than that of Re(III) leads to smaller $d_\sigma-d_\sigma$ overlap of **2b** than that of **1**. These two factors are responsible to the weaker σ bonding interaction of **2b** than that of **1**.

It is of considerable interest to make a comparison between **2a** and **2b**, because the electronic structure is much different despite the similar geometry and similar d electron number; both complexes take the face-sharing structure and **2b** has fewer d electrons than **2a** by only one. In **2a**, the main configuration is $\sigma^2\delta^4\delta^{*1}$. It is expected that one d electron is lost from the δ^* orbital upon going to **2b** from **2a** and the Re−Re bond of **2b** is stronger than that of **2a**. However, natural orbital population of the δ orbital extremely decreases and that of the δ^* orbital rather increases in **2b**, as shown in Table 2, against the above expectation. These population changes suggest that one d electron is lost not from the δ^* orbital but from the δ orbital. Thus, the electronic structure of **2b** cannot be understood in terms of a usual orbital picture. Also, it is noted that the Re−Re bond distance becomes longer in **2b** than in **2a**, as shown in Table S1 (Supporting Information). One plausible reason of the longer Re−Re distance in **2b** is that one electron loss occurs in the δ orbital upon going to **2b** from **2a**. This induces weakening of the δ bonding interaction. It is worthwhile to discuss the reason that one electron loss occurs not in the δ^* orbital but in the δ orbital in **2a**. It is likely that the electron repulsion of the d-shell is larger in **2b** than in **2a** because the d orbital of the Re(IV)−Re(IV) core is more compact than that of the Re(III)−Re(IV) core. Also, Coulomb repulsion in the d-shell is larger in the $\sigma^2\delta^4$ configuration than in the $\sigma^2\delta^3\delta^{*1}$ configuration. If the energy separation between the δ and δ^* orbitals is sufficiently large, one δ^* electron loss occurs in the $\sigma^2\delta^4\delta^{*1}$ configuration to afford the $\sigma^2\delta^4$ configuration upon going to **2b** from **2a**. In these complexes, however, the $\delta-\delta^*$ energy separation is small. Thus, one δ electron loss occurs in the $\sigma^2\delta^4\delta^{*1}$ configuration to afford the $\sigma^2\delta^3\delta^{*1}$ configuration, so as to decrease Coulomb repulsion in the d-shell.

The DFT(B3LYP), CCSD, CCSD(T), BS-DFT(B3LYP), BS-CCSD, and BS-CCSD(T) methods were also applied to **2b**, as shown in Table 3. The $^5A_1'$ state is evaluated to be more stable than the $^1A_1'$ state by the methods other than BS-DFT(B3LYP). These results are different from the results by the MRMP2 calculations.[39] On the other hand, the DFT(B3LYP) method presents a similar result by the MRMP2 calculation, which indicates that the DFT(B3LYP) method is useful to present correctly the ground state of **2b**.

3.3. Edge-Sharing Complex, $[Re_2(\mu\text{-}Cl)_2Cl_8]^{2-}$ (3). Relative energies and natural orbital populations of the ^1A_g, $^3B_{1u}$, ^5A_g, and $^7B_{1u}$ states were calculated by the CASSCF/basis II and MRMP2/basis II methods, as shown in Table 2; almost the same results are calculated with basis I (see Supporting Information Table S3). In all these states, the populations of the σ, π, and δ bonding orbitals are almost the same as those of their antibonding counterparts, respectively. This means that the σ, π, and δ bonding interactions do not contribute to the Re−Re bond in these four states. The weights of several important electron configurations are evaluated to be very small by the CASSCF method; 6% for both the $\sigma^2\pi^2\delta^2$ and $\sigma^2\pi^2\delta^{*2}$ configurations in the ^1A_g state, 7% for both the $\sigma^2\pi^2\delta^1\delta^{*1}$ and $\sigma^2\delta^1\delta^{*1}\pi^{*2}$ configurations in the $^3B_{1u}$ state, and 16% for both the $\sigma^2\pi^1\delta^1\delta^{*1}\pi^{*1}$ and $\pi^1\delta^1\delta^{*1}\pi^{*1}\sigma^{*2}$ configurations in the ^5A_g state. As a result, these four states are in almost the same energy (within 0.03 eV). In other words, the low spin state is not stabilized by the Re−Re bonding interaction unlike **1**, **2a**, and **2b**. These results are consistent with the experimental report that **3** is not diamagnetic but paramagnetic.[12]

The absence of the Re−Re bonding interaction arises from the long Re−Re distance (3.691 Å) due to the edge-sharing geometry. The oxidation state of Re(IV) center is also responsible for the absence of the Re−Re bonding interaction, as follows: Because the d orbital of Re(IV) expands less than that of Re(III), the σ, π, and δ bonding interactions in **3** are weaker than those in **1**. For instance, the population of the σ orbital is almost the same as that of the σ^* orbital in those four states of **3**, as shown in Table 2, whereas the population of the σ orbital (1.30) is considerably larger than that of the σ^* orbital in the $^1A_{1g}$ state of **1** at the same Re−Re distance (3.691Å) (see Figure 2a). These results clearly show that the σ bonding interaction disappears in **3** but still remains in **1** at r(Re−Re) = 3.691 Å.

Three d electrons are localized in three d orbitals of each Re center because the Re−Re interaction is absent. As a result, the four states, ^1A_g, $^3B_{1u}$, ^5A_g, and $^7B_{1u}$, emerge from the electron configurations in which six electrons occupy the σ, π, δ, δ^*, π^*, and σ^* orbitals in D_{2h} symmetry. The other states are at much higher energy than these four states by over 1.0 eV (see Table S5 in Supporting Information) because those states consist mainly of the high-energy excited configurations.

4. Conclusions

Four dinuclear rhenium complexes, **1**, **2a**, **2b**, and **3**, were theoretically investigated by the CASSCF, MRMP2, SA-CASSCF, and MCQDPT methods. In the $^1A_{1g}$ ground state of **1**, the weights of the $\sigma^2\pi^4\delta^2$ and $\sigma^2\pi^4\delta^{*2}$ configurations are 67 and 18%, respectively, where weights evaluated by either the

CASSCF/basis II or the SA-CASSCF/basis II method are presented hereafter. The energy difference between the $^1A_{1g}$ and $^3A_{2u}$ states, which corresponds to the approximate stabilization energy by the δ bonding interaction, is evaluated to be 0.52 eV by the MRMP2/basis II method. The $^7A_{2u}$ state is much less stable than the $^3A_{2u}$ state by 5.77 eV. This is because the bonding interactions of the two π orbitals disappear upon going to the $^7A_{2u}$ state from the $^3A_{2u}$ state. The $^9A_{1g}$ state is further less stable than the $^7A_{2u}$ state by 4.36 eV because the σ bonding interaction disappears upon going to the $^9A_{1g}$ state from the $^7A_{2u}$ state. Thus, the σ, π, and δ bonding interactions yield the approximate stabilization energies of 4.36, 2.89 (=5.77/2), and 0.52 eV, respectively. In the $^1A_{1g}$ state, the δ bonding interaction completely disappears at r(Re−Re) = 3.6 Å, whereas the π and σ bonding interactions completely disappear at r(Re−Re) = 4.6 and 6.0 Å, respectively.

In the $^2E''$ ground state of **2a**, the weights of the $\sigma^2\delta^4\delta^{*1}$ and $\sigma^2\delta^3\delta^{*2}$ configurations are 72 and 12%, respectively. The natural orbital populations clearly show that the δ bonding interaction in the $^4E'$ state is much weaker than that in the $^2E''$ state. As a result, the former state is evaluated to be 0.36 eV less stable than the latter one. These results indicate that the δ bonding interaction is weaker in **2a** than in **1**. In the $^1A_1'$ ground state of **2b**, the weight of the $\sigma^2\delta^4$ configuration is evaluated to be 18%. The energy difference between the $^1A_1'$ and $^5A_1'$ states is evaluated to be 0.21 eV by the MRMP2/basis II method, which corresponds to the approximate stabilization energy by the two components of degenerate δ bonding interactions. The σ bonding interaction is also weak in this complex, as follows: In the $^5A_1'$ state, the weights of the $\sigma^2\delta^2\delta^{*2}$ and $\delta^2\delta^{*2}\sigma^{*2}$ configurations are 73 and 11%, respectively. The energy difference between the $^5A_1'$ and $^7A_2''$ states is evaluated to be 1.73 eV by the MRMP2/basis II method, which corresponds to the approximate stabilization energy by the σ bonding interaction. This approximate stabilization energy is much smaller than that of **1**. The bonding nature and the electronic structure of **2b** are much different from the expectation based on a usual orbital picture that one d electron is lost from the δ^* orbital upon going to **2b** from **2a** and the δ bonding interaction becomes stronger in **2b**. However, our theoretical calculation presents completely different results from the above expectation; the natural orbital population of the δ orbital decreases by 1.29 and that of the δ^* orbital increases by 0.29, which indicates that one electron loss occurs not in the δ^* orbital but in the δ orbital upon going to **2b** from **2a**. These unexpected results are interpreted in terms that one electron loss occurs in the δ orbital so as to decrease Coulomb repulsion in the d-shell because the $\delta-\delta^*$ energy separation is very small.

In **3**, the σ, π, and δ bonding interactions do not contribute to the Re−Re bond. As a result, the low spin ^1A_g state is not stabilized by these bonding interactions unlike **1**, **2a**, and **2b**. Four states, ^1A_g, $^3B_{1u}$, ^5A_g, and $^7B_{1u}$, are in almost the same energy within 0.03 eV. This result is consistent with the experimental report that **3** is paramagnetic.[12]

The above-mentioned energy difference between the ground and low-energy excited states lead to the conclusion that the Re−Re bonding interactions in the order **1** > **2a** > **2b** ≫ **3**, which is interpreted in terms of the Re−Re distance and the Re oxidation state.

Acknowledgment. This work was financially supported by Grant-in-Aids on basic research (No. 15350012), Priority Areas for "Reaction Control of Dynamic Complexes" (No.420), Creative Scientific Research, and NAREGI Project from the Ministry of Education, Science, Sports, and Culture. Some of theoretical calculations were performed with SGI workstations of Institute for Molecular Science (Okazaki, Japan), and some of them were carried out with PC cluster computers of our laboratory.

Supporting Information Available: The experimental geometries of **1**, **2a**, **2b**, and **3** used for calculations (Table S1). Relative energies and natural orbital populations of **1** calculated with the MRMP2/basis I and MRMP2/basis II optimized geometries (Table S2). Relative energies and natural orbital populations of **1**, **2a**, **2b**, and **3** calculated by basis I with experimental geometries (Table S3). Weights of electron configurations of the ground states of **1**, **2a**, **2b**, and **3** (Table S4). Relative energies and natural orbital populations of various electronic states of **3** (Table S5). Natural orbital populations of **2a**, **2b**, and **3** by the CAS-CI method using much larger active space (Table S6). Comparisons of basis I and II in the calculations of the PE curves (Table S7 and Figure S1). Several important Re−Re and Re−Cl−Re orbitals of **2a** and **2b** (Scheme S1) and **3** (Scheme S2). This material is available free of charge via the Internet at http://pubs.acs.org.

References and Notes

(1) (a) Cotton, F. A.; Harris, C. B. *Inorg. Chem.* **1965**, *4*, 330. (b) Cotton, F. A. *Inorg. Chem.* **1965**, *4*, 334.
(2) Brencic, J. V.; Cotton, F. A. *Inorg. Chem.* **1969**, *8*, 7.
(3) Cotton, F. A.; Daniels, L.; Davison, A.; Orvig, C. *Inorg. Chem.* **1981**, *20*, 3051.
(4) Cotton, F. A.; Bratton, W. K. *J. Am. Chem. Soc.* **1965**, *87*, 921.
(5) Heath, G. A.; McGrady, J. E.; Raptis, R. G.; Willis, A. C. *Inorg. Chem.* **1996**, *35*, 6838.
(6) Hauck, H. G.; Klingelhöfer, P.; Müller, U.; Dehnicke, K. *Z. Anorg. Allg. Chem.* **1984**, *510*, 180.
(7) Baranov, A. I.; Khvorykh, G. V.; Troyanov, S. I. *Z. Anorg. Allg. Chem.* **1999**, *625*, 1240.
(8) Kistenmacher, T. J.; Stucky, G. D. *Inorg. Chem.* **1971**, *10*, 122.
(9) Wessel, G. J.; Ijdo, D. J. W. *Acta Crystallogr.* **1957**, *10*, 466.
(10) Saillant, R.; Jackson, R. B.; Streib, W. E.; Folting, K.; Wentworth, R. A. D. *Inorg. Chem.* **1971**, *10*, 1453.
(11) Watson, W. H., Jr.; Waser, J. *Acta Crystallogr.* **1958**, *11*, 689.
(12) Beck, J.; K.-Buschbaum, M.; Wolf, F. *Z. Anorg. Allg. Chem.* **1999**, *625*, 975.
(13) Khvorykh, G. V.; Troyanov, S. I.; Baranov, A. I.; Serov, A. A. *Z. Anorg. Allg. Chem.* **1998**, *624*, 1026.
(14) Mucker, K.; Smith, G. S.; Johnson, Q. *Acta Crystallogr.* **1968**, *B24*, 874.
(15) Bursten, B. E.; Cotton, F. A.; Fanwick, P. E.; Stanley, G. G.; Walton, R. A. *J. Am. Chem. Soc.* **1983**, *105*, 2606.
(16) Hay, P. J. *J. Am. Chem. Soc.* **1982**, *104*, 7007.
(17) Blaudeau, J.-P.; Ross, R. B.; Pitzer, R. M. *J. Phys. Chem.* **1994**, *98*, 7123.
(18) Gagliardi, L.; Roos, B. O. *Inorg. Chem.* **2003**, *42*, 1599.
(19) (a) Cowman, C. D.; Gray, H. B. *J. Am. Chem. Soc.* **1973**, *95*, 8177. (b) Trogler, W. C.; Gray, H. B. *Acc. Chem. Res.* **1978**, *11*, 1. 232.
(20) (a) McGrady, J. E.; Stranger, R.; Lovell, T. *J. Phys. Chem. A* **1997**, *101*, 6265. (b) McGrady, J. E.; Lovell, T.; Stranger, R. *Inorg. Chem.* **1997**, *36*, 3242. (c) McGrady, J. E.; Stranger, R.; Lovell, T. *Inorg. Chem.* **1998**, *37*, 3802. (d) Stranger, R.; Lovell, T. McGrady, J. E. *Inorg. Chem.* **1999**, *38*, 5510. (e) Stranger, R.; Turner, A.; Delfs, C. D. *Inorg. Chem.* **2001**, *40*, 4093. (f) Cavigliasso, G.; Stranger, R. *Inorg. Chem.* **2004**, *43*, 2368. (g) Petrie, S.; Stranger, R. *Inorg. Chem.* **2004**, *43*, 2597. (h) Cavigliasso, G.; Comba, P.; Stranger, R. *Inorg. Chem.* **2004**, *43*, 6734. (i) Cavigliasso, G.; Stranger, R. *Inorg. Chem.* **2005**, *44*, 5081.
(21) (a) Hirao, K. *Chem. Phys. Lett.* **1992**, *190*, 374. (b) Hirao, K. *Chem. Phys. Lett.* **1992**, *196*, 397. (c) Hirao, K. *Int. J. Quantum Chem.* **1992**, *Symp. 26*, 517.
(22) (a) Nakano, H. *J. Chem. Phys.* **1993**, *99*, 7983. (b) Nakano, H. *Chem. Phys. Lett.* **1993**, *207*, 372.
(23) (a) Becke, A. D. *Phys. Rev. A* **1988**, *38*, 3098. (b) Becke, A. D. *J. Phys. Chem.* **1993**, *98*, 5648.
(24) Lee, C.; Yang, W.; Parr, R. G. *Phys. Rev. B* **1988**, *37*, 785.
(25) Hay, P. J.; Wadt, W. R. *J. Chem. Phys.* **1985**, *82*, 299.
(26) Couty, M.; Hall, M. B. *J. Comput. Chem.* **1996**, *17*, 1359.
(27) Ehlers, A. W.; Böhme, M.; Dapprich, S.; Gobbi, A.; Höllwarth, A.; Jonas, V.; Köhler, K. F.; Stegmann, R.; Veldkamp, A.; G. Frenking. *Chem. Phys. Lett.* **1993**, *208*, 111.

(28) Woon, D. E.; Dunning, T. H., Jr. *J. Chem. Phys.* **1993**, *98*, 1358.

(29) Complexes **2a**, **2b**, and **3** were also investigated by the CAS-CI calculations here. These calculations present almost the same natural orbital populations as those of either CASSCF or SA-CASSCF calculation, indicating that the active spaces adapted here are reasonable; see Supporting Information Table S6, Scheme S1, and Scheme S2.

(30) Schmidt, M. W.; Baldridge, K. K.; Boatz, J. A.; Albert, S. T.; Gordon, M. S.; Jensen, J. J.; Koseki, S.; Matsunaga, N.; Nguyen, K. A.; Su, S.; Windus, T. L.; Dupuis, M.; Montgomery, J. A. *J. Comput. Chem.* **1993**, *14*, 1347.

(31) Nakano, H. *MR2D*, version 2.0; University of Tokyo: Tokyo, Japan, 1995.

(32) Frisch, M. J.; Trucks, G. W.; Schlegel, H. B.; Scuseria, G. E.; Robb, M. A.; Cheeseman, J. R.; Montgomery, J. A., Jr.; Vreven, T.; Kudin, K. N.; Burant, J. C.; Millam, J. M.; Iyengar, S. S.; Tomasi, J.; Barone, V.; Mennucci, B.; Cossi, M.; Scalmani, G.; Rega, N.; Petersson, G. A.; Nakatsuji, H.; Hada, M.; Ehara, M.; Toyota, K.; Fukuda, R.; Hasegawa, J.; Ishida, M.; Nakajima, T.; Honda, Y.; Kitao, O.; Nakai, H.; Klene, M.; Li, X.; Knox, J. E.; Hratchian, H. P.; Cross, J. B.; Bakken, V.; Adamo, C.; Jaramillo, J.; Gomperts, R.; Stratmann, R. E.; Yazyev, O.; Austin, A. J.; Cammi, R.; Pomelli, C.; Ochterski, J. W.; Ayala, P. Y.; Morokuma, K.; Voth, G. A.; Salvador, P.; Dannenberg, J. J.; Zakrzewski, V. G.; Dapprich, S.; Daniels, A. D.; Strain, M. C.; Farkas, O.; Malick, D. K.; Rabuck, A. D.; Raghavachari, K.; Foresman, J. B.; Ortiz, J. V.; Cui, Q.; Baboul, A. G.; Clifford, S.; Cioslowski, J.; Stefanov, B. B.; Liu, G.; Liashenko, A.; Piskorz, P.; Komaromi, I.; Martin, R. L.; Fox, D. J.; Keith, T.; Al-Laham, M. A.; Peng, C. Y.; Nanayakkara, A.; Challacombe, M.; Gill, P. M. W.; Johnson, B.; Chen, W.; Wong, M. W.; Gonzalez, C.; Pople, J. A. *Gaussian 03*, revision C.02; Gaussian, Inc.: Wallingford, CT, 2004.

(33) (a) Flükiger, P.; Lüthi, H. P.; Portmann, S.; Weber, J. *MOLEKEL*, version 4.3; Scientific Computing: Manno, Switzerland, 2000−2002. (b) Portmann, S.; Lüthi, H. P. *CHIMIA* **2000**, *54*, 766.

(34) The bond order is defined in usual way: bond order = {(sum of the natural orbital populations of bonding orbitals) − (sum of the natural orbital populations of antibonding orbitals)}/2.

(35) The stabilization energy by the δ bonding interaction corresponds to the energy difference between the $^1A_{1g}$ and $^3A_{2u}$ states when orbital relaxation is negligibly small. Because this relaxation occurs more or less, the energy difference is not exactly the same as the stabilization energy by the δ bonding interaction. However, it is likely that the energy difference approximately corresponds to the stabilization energy by the δ bonding interaction, because the orbital relaxation is not large, as suggested by almost the same populations of σ, σ^*, π, and π^* orbitals between the $^1A_{1g}$ and $^3A_{2u}$ states.

(36) Incorporation of spin−orbit coupling interaction is necessary for highly quantitative discussion, as reported by Gagliardi and Roos.[18] It is likely that semiquantitatively reliable discussion is presented here about the stabilization energies by the σ, π, and δ bonding interactions, at least, because the spin−orbit coupling is mainly one-center interaction.

(37) The $^7A_{2u}$ and $^9A_{1g}$ states were calculated here to evaluate the strengths of the σ, π, and δ bonding interactions from the energy differences among the $^1A_{1g}$, $^3A_{2u}$, $^7A_{2u}$, and $^9A_{1g}$ states.

(38) The energy stabilization of each state relative to the very long Re−Re distance (6.0 Å) slightly increases upon going to basis II from basis I, suggesting that the basis set super position error would not be very large; see Figure S1 and Table S7 in Supporting Information.

(39) This is probably because the multiconfigurational nature is strong in this complex. The BS methods should be carefully applied to estimation of energy difference between the ground and low-energy excited states when they exhibit multiconfigurational nature.